AIP Advances

Optical bistability in side-mode injection locked dual-mode Fabry-Pérot laser diode

Jian Wei Wu, Bikash Nakarmi, Tran Quoc Hoai, and Yong Hyub Won

Citation: AIP Advances **3**, 082109 (2013); doi: 10.1063/1.4818274
View online: http://dx.doi.org/10.1063/1.4818274
View Table of Contents: http://scitation.aip.org/content/aip/journal/adva/3/8?ver=pdfcov
Published by the AIP Publishing

Optical bistability in side-mode injection locked dual-mode Fabry-Pérot laser diode

Jian Wei Wu,[1,a] Bikash Nakarmi,[2] Tran Quoc Hoai,[2] and Yong Hyub Won[1]
[1]*Department of Electrical Engineering, Korea Advanced Institute of Science and Technology, Daejeon 305-714, Republic of Korea*
[2]*Department of Information and Communication Engineering, Korea Advanced Institute of Science and Technology, Daejeon 305-714, Republic of Korea*

(Received 1 February 2013; accepted 30 July 2013; published online 6 August 2013)

In this paper, optical bistability characteristics are demonstrated experimentally based on a dual-mode laser system comprising a multi-mode Fabry-Pérot laser diode (MMFP-LD) and a built-in feedback cavity formed by a fiber facet. The results show that two lasing modes with frequency separation of ~0.58 THz and comparable peak powers can be achieved by judicious adjustment of the bias current and the operating temperature of the laser chip, which has a peak fluctuation of less than ~1 dBm over a measurement period of one hour. A combination of appropriate external injection power and wavelength detuning can result in remarkable optical bistability in two oscillation modes, in which the resulting contrast ratio between the unlocked and locked states can be up to 30 dB, and the corresponding hysteresis loop width can be changed by controlling the side-mode injection power and the wavelength detuning. [http://dx.doi.org/10.1063/1.4818274]

I. INTRODUCTION

Dual-mode laser systems have attracted considerable attention because of their numerous potential applications, including terahertz frequency generation,[1–5] THz imaging,[6] microwave/millimeter wave generation,[7–10] optical memory,[11–14] dual-wavelength interferometry,[15–17] and optical switching.[18] To date, many techniques have been proposed and experimentally demonstrated to successfully produce dual-mode lasing operation,[19–24] and among these, multi-mode Fabry-Pérot laser diode (MMFP-LD) based devices are worthy of extensive investigation because of their rich variety of nonlinear phenomena, cost effectiveness, low power consumption and low threshold current.[25–27] In general, the MMFP-LDs associated with external cavity feedback and incorporating fiber Bragg gratings and tunable filters were often chosen for selection of special feedback wavelengths that are then fed back into the active region to produce dual-mode laser oscillation in the output spectrum. These previously presented techniques undoubtedly have some distinct advantages and some limitations in terms of optical signal processing. In recent years, a very compact laser device consisting of an MMFP-LD that uses a built-in external cavity produced by a fiber facet has been presented and was experimentally shown to achieve single-mode lasing operation with a high side-mode suppression ratio (SMSR) by our research group.[28] Single mode output is easily achieved by adjusting the bias current and operating temperature, such that this lasing system is generally known as the single-mode Fabry-Pérot laser diode (SMFP-LD), and it has already been applied to various optical functions, including wavelength conversion,[29] logic gates,[30] flip-flops[31] and switching[32] because of its prominent properties, including self-locking ability, a wide tunable range, the high SMSR, and its compact configuration. However, in a recent experiment, we

[a]Author to whom correspondence should be addressed. Electronic mail: jwwu@kaist.ac.kr

were surprised to find that the predominantly SMFP-LD can cause two lasing modes to oscillate simultaneously in the laser cavity by judicious adjustment of the injection current and the operating temperature of the active region. Naturally, some of the characteristics of the resulting dual-mode lasing spectrum are similar to those of the single mode operation case of the SMFP-LD. However, in reality, we found it to be a little difficult to produce dual-mode operation with a high SMSR and peak levels that are comparable to those of the effective single mode output that can be generated easily in most cases with the SMFP-LD; it should also be noted that the power fluctuation in single mode operation is smaller than that of the two modes in dual mode operation. To avoid confusion between the concepts of the single-mode and dual-mode lasers, the dual-mode Fabry-Pérot laser diode (DMFP-LD) is defined for two-mode oscillation in the MMFP-LD using a built-in external cavity for this study.

Compared with previously reported two-mode lasing technologies,[33–35] the DMFP-LD presented in this work has some distinctly competitive abilities, including low bias current, low power consumption, and a compact configuration for application to optical communications. Also, previous research indicates that the optical bistability induced by the side-mode injected power should prove to be a very significant phenomenon for dual-mode lasing systems, which have been used directly in optical memory and flip-flop technologies. Therefore, we will focus on observation and discussion of the optical bistability hysteresis characteristics in this study, where, when both the externally injected power and the wavelength detuning, defined as the difference between the injected wavelength and the adjacent side mode peak, are changed, the device exhibits significant optical bistability hysteresis, in which the loop width is strongly dependent on the input power and the corresponding wavelength detuning. On the basis of this investigation, we believe that potential applications such as optical memory, optical wavelength conversion, and optical switching using optical bistability based on the proposed DMFP-LD system can be explored and demonstrated.

II. EXPERIMENTAL SETUP AND PRINCIPLE

The experimental setup for observation of the optical bistability caused by the injected power and wavelength detuning is depicted schematically in Fig. 1(a), where the polarization state of the continuous wave generated by the tunable laser (TL) can be controlled by the polarization controller (PC). To perform the injection locking effectively, an output beam with a TE polarization state is required, with a power level that can be controlled by adjusting the variable optical attenuator (VOA) before it enters the DMFP-LD. The output power from the VOA is divided equally into the power meter and the circulator by using a 50:50 fiber coupler, meaning that half of the energy can be captured by the power meter to indirectly measure the injected power for the DMFP-LD, while the remaining energy is introduced into the DMFP-LD via the circulator to produce the injection locking behavior in the active region. The resulting response of the dual-mode laser to the injected beam can be observed using the optical spectrum analyzer (OSA). In the experiment, the most important element is the DMFP-LD, which is depicted schematically in Fig. 1(b), and which comprises an MMFP-LD that incorporates an external cavity formed by a fiber facet. Some special lasing modes can be selected as feedback beams by the fiber facet in the external cavity, where, if only one feedback mode is achieved, the lasing configuration is the well-known SMFP-LD; however, if two reflected lasing modes are fed back into the laser chip, leading to simultaneous oscillation in the external cavity and chip, it becomes the DMFP-LD presented in this work. The detailed design parameters and physical mechanisms for this laser setup can be found in the previous report,[28] in which the single mode oscillation that can be easily achieved by tuning the operation current and temperature is discussed. As such, dual-mode emission can also be attained by precisely adjusting the crucial parameters including current and temperature based on the same laser device, whose operation principle, spectrum characteristic and bistability behavior are presented and discussed in this study.

As shown in Fig. 2, lasing modes located in the gain bandwidth that simultaneously match the oscillation conditions of the laser and the external cavity can obtain sufficient gain to lead to laser emission. Therefore, by strict tuning of the corresponding bias current and operating temperature, we can cause only the two lasing modes shown in Fig. 2 to attain sufficient stimulated emission,

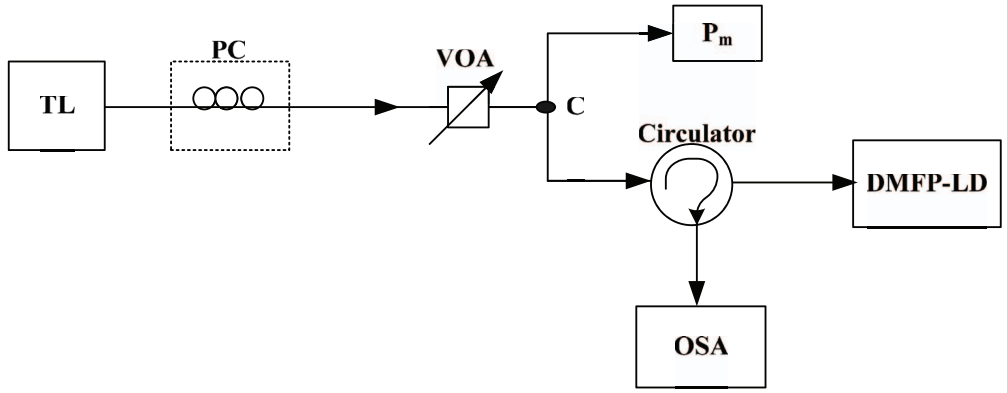

(a)

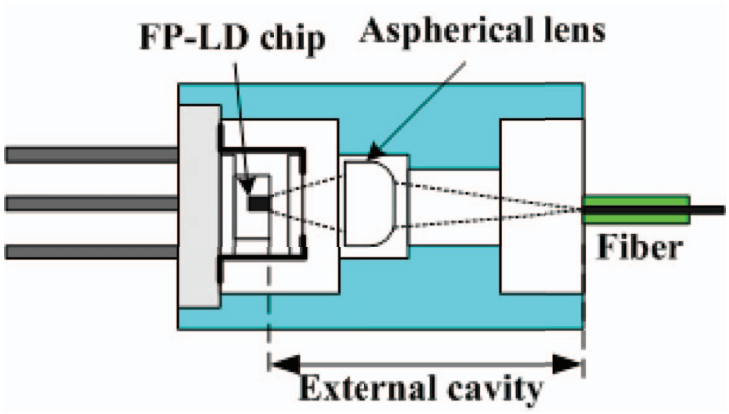

(b)

FIG. 1. (a) Experimental setup for observation of optical bistability based on DMFP-LD. TL: tunable laser. PC: polarization controller. VOA: variable optical attenuator. C: coupler (50:50). Pm: power meter. DMFP-LD: dual-mode Fabry-Pérot laser diode. OSA: optical spectrum analyzer. (b) Schematic of MMFP-LD structure with a built-in external cavity configuration.

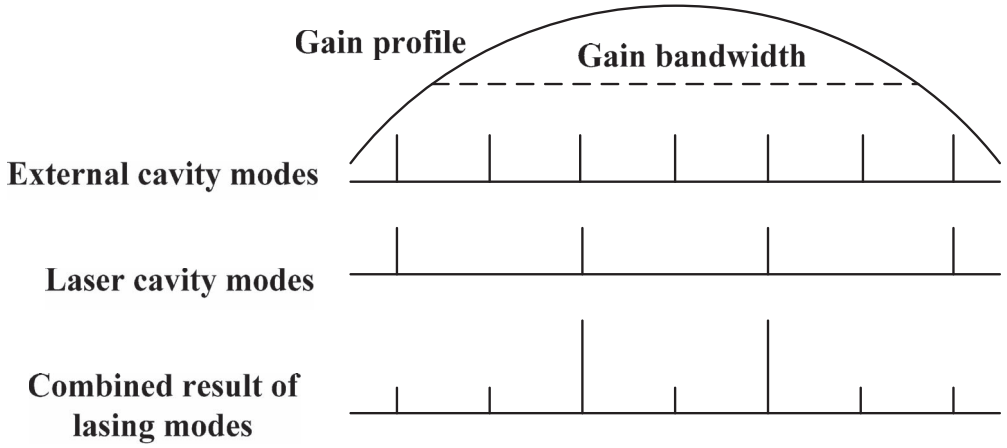

FIG. 2. Schematic of lasing modes for generation of dual-mode lasing oscillation based on the DMFP-LD.

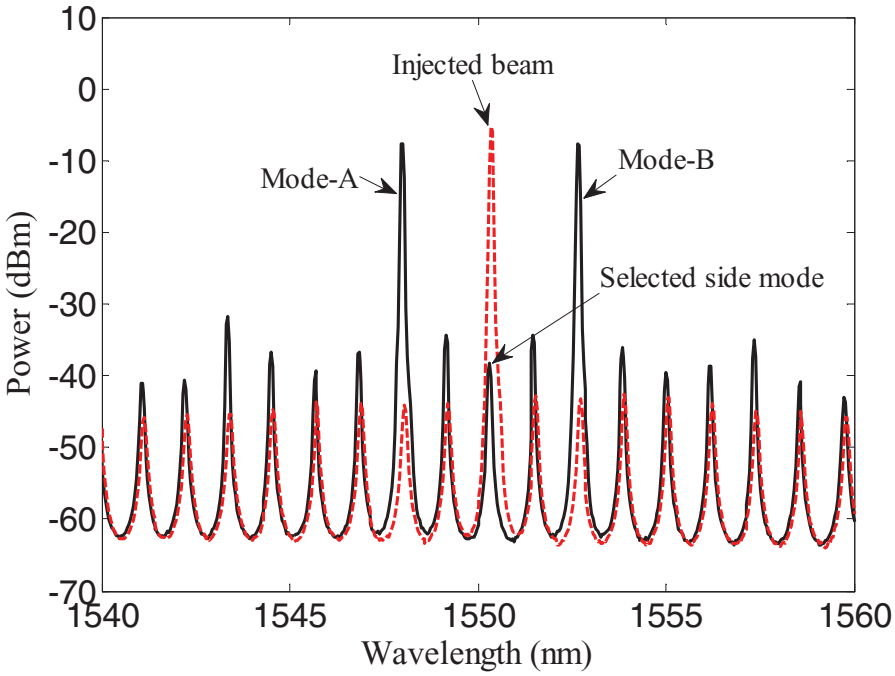

FIG. 3. Optical spectra for free running dual-mode emission (black solid line), and for the injection locking case (red dashed line).

while the other lasing modes are highly suppressed, with the result that dual-mode laser output is produced by the device. The corresponding experimental spectrum captured by the OSA is plotted for a bias current of 17 mA at an operating temperature of 21.3 °C in Fig. 3, where the two generated modes (designated mode-A and mode-B) have an SMSR of around 24 dB and comparable peak levels for the free running case. The frequency separation between mode-A and mode-B is as large as ∼0.58 THz, corresponding to the spacing of four fundamental FP-LD modes, so that the two emission modes have a weak coupling effect that leads to a more stable lasing output. Figure 4 illustrates the fluctuations of the peak wavelength and the power level with respect to the operating time, in which the emitted lasing wavelength is very stable, and a peak power variation of less than 1 dBm is observed as a result of the weak interaction and mode competition between the two lasing modes.

To further understand the presented dual-mode emission, some noticeable issues are, specially, pointed out that, (1) In the DMFP-LD, the emitted dual-mode wavelengths are strongly dependent on the combination of injection current and operation temperature in active region, i.e., either the injection current or operation temperature is changed, the generated oscillation wavelengths will be also shifted. (2) For a special DMFP-LD in the experiment, it is obvious that the gain bandwidth and corresponding laser structure including the cavity length are determined. Therefore, the wavelength separation between oscillation modes is nearly fixed, and only the emission wavelengths are shifted in the case of different combination of current and temperature, which can be red-shifted (blue-shifted) by increasing (reducing) the operating temperature. In general, the output oscillation modes are located at the center of emitted spectrum resulting from the laser gain. (3) Through the investigation, one can know that the tolerances for bias current and temperature are very small, i.e., the stability range for generating two modes emission is very sensitive to the change of temperature and current. In the experiment, one can achieve dual-mode oscillation by judiciously adjusting the current (temperature) under the condition of a fixed temperature (current).

In the injection locking case, the external injection wavelength should be slightly longer than the peak wavelength of the selected side mode to enable easy observation of the locking behavior. Hence, after an injected beam with enough high peak level is introduced into the laser chip, the

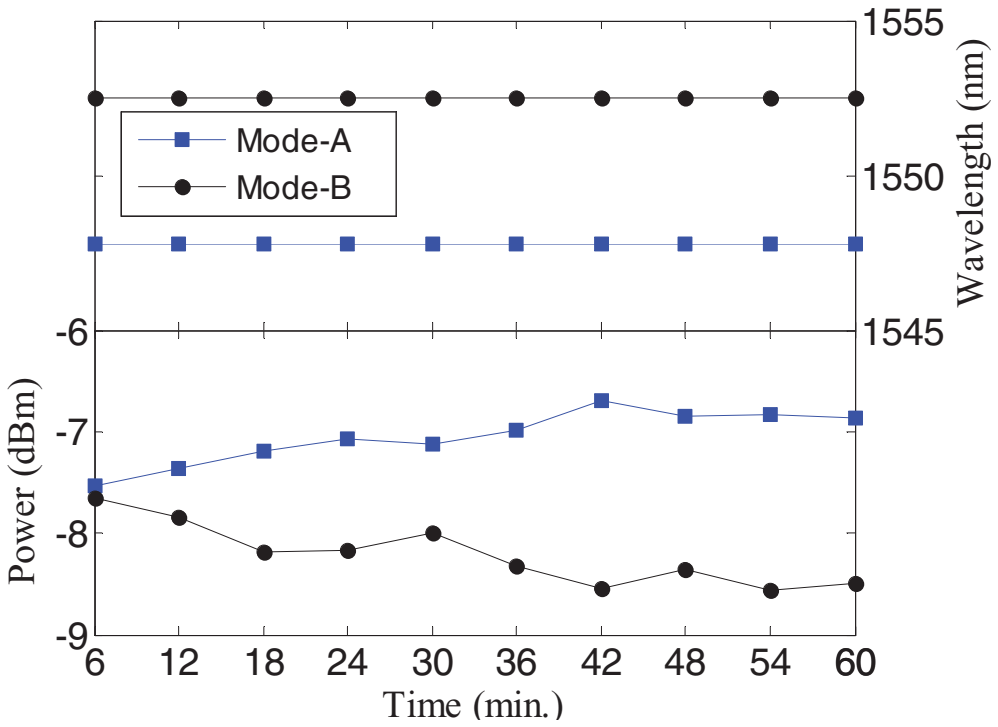

FIG. 4. Variation of peak wavelength and power level for two emitted oscillation modes within one hour.

lasing modes are highly suppressed because of the reduction in free carriers that is attributed to the strong stimulation emission induced by external injection beam; as a result, the refractive index in the active region is remarkably enhanced resulting from the free carrier depletion caused by the strong stimulated emission so that the total lasing spectrum is red-shifted with the result that the output lasing mode is locked at the injected wavelength. The outcome injection locking spectrum is shown as a red dashed line in Fig. 3. To clearly show the evolution of the injection locking process induced by the external input power, Fig. 5 plots the peak power levels of mode-A, mode-B, and a selected side mode as a function of the injected power, for which wavelength detuning of 0.16 nm is determined. As the figure shows, when the injection power is at a low level, both mode-A and mode-B can still hold comparable peak power levels as a result of the weak stimulated emission induced by external injection power. However, as the input power increases to ∼−7 dBm, a surprising phenomenon was noted for mode−A, where its peak level begins to decay slowly. In contrast, the peak of mode-B shows almost no variation until the input power is increased to ∼2.9 dBm, which can suppress mode-A to the ∼−28.5 dBm level. It is also easily understood that the selected side mode power is linearly enhanced when the input power is increased from ∼−31 dBm to ∼2.9 dBm. Another obvious issue is that, although the mode-A peak obtains high suppression, the peak wavelengths of the two lasing modes are still not shifted when the injection power is less than ∼2.9 dBm. One can think that the power decay of mode-A should mainly be attributed to mode competition caused by the externally injected beam in the case where the input power is below ∼2.9 dBm. In contrast, when the injection peak overruns ∼2.9 dBm, both lasing modes are simultaneously heavily suppressed because of reduction in free carrier resulting from strong stimulation emission caused by the high intensity injection, with the result that the output laser is locked at an injected wavelength associated with the red shift of the other lasing modes. The resulting SMSR shown in Fig. 5 is up to 30 dB in the injection locking case. In our experiment, we also found that similar results can be obtained by selecting different side modes in the free running spectrum. Because of gain bandwidth limitations, the spacing between the two oscillation modes is effectively determined for the various two mode oscillation cases that can be observed by precisely selecting other combination of injection current and operating temperature in the laser chip.

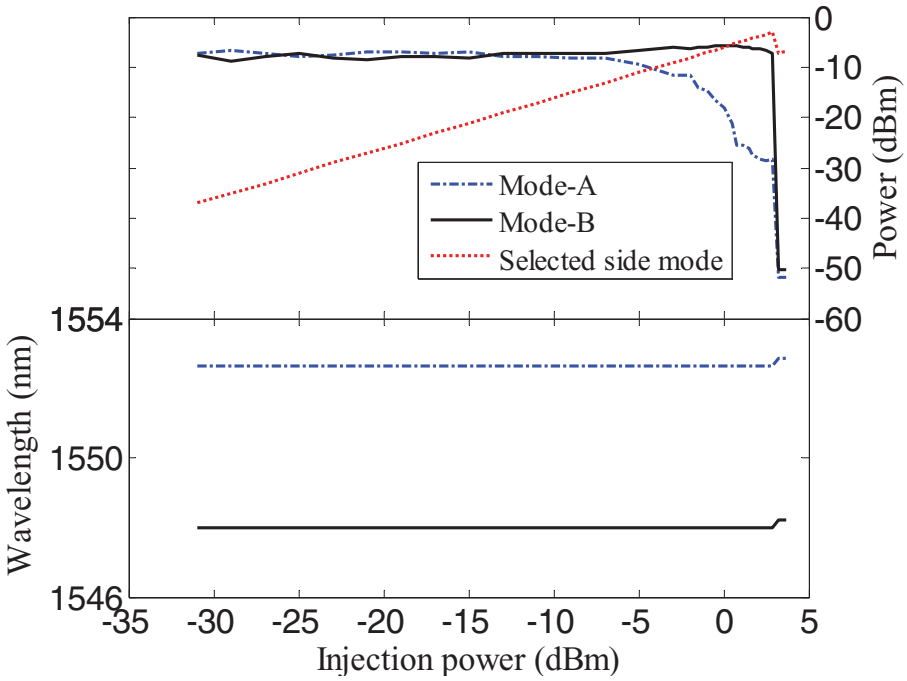

FIG. 5. Peak evolution of mode-A, mode-B, and a selected side mode versus the injection power.

III. OPTICAL BISTABILITY

Optical bistability, which produces two output states for a single input state, is a very important nonlinear process in FP-LDs with optical feedback, and has been observed and applied extensively in various optical technologies.[36–38] In comparison to previous reports, the bistability hysteresis produced by the dual-mode laser system presented here also has some significant properties that can be seen in Fig. 6, where the input-output power relationship shows remarkable bistable hysteresis loops for mode-A, mode-B and the selected side mode for various wavelength detuning levels. First, we focus on the case of mode-A, as shown in Fig. 6(a). During the gradual injection locking process, the peak of mode-A first experiences oscillation behavior, where the power begins to decay slowly with increasing injected power. This implies that the output power of mode-A has some fluctuation as the externally injected power is gradually increased, which is more sensitive to the variation of external injection power. It should also be noted that the oscillation behavior becomes more pronounced for larger wavelength detuning case, in which one can think that the enhanced fluctuation behavior in mode-A should be related to the fact that a higher threshold power is required to reach full injection locking state in outcome spectrum. These results can be confirmed by the plot, where it is clearly shown that the required threshold power for injection locking is lowest for the wavelength detuning level of 0.04 nm rather than the other two wavelength detuning cases of 0.08 and 0.12 nm, and the output power fluctuation of mode-A is considerably enhanced by increased wavelength detuning. Another issue should also be noted here with regard to the clockwise hysteresis loop shown in Fig. 6(a), where the loop width is compressed to a minimum in the 0.08 nm wavelength detuning case, but is obviously broadened for the wavelength detuning of 0.04 nm. In the case of mode-B, the properties of the bistability loop obtained, including the loop width and the hysteresis direction, are similar to those of the case of mode-A for corresponding wavelength detuning levels, as shown in Fig. 6(b), although the oscillation behavior in the output power has nearly disappeared. This is because, after the introduction of the side mode injected beam, the influence of mode competition on mode-B is only very slight before full injection locking occurs. As a result, the obtained contrast ratios between the unlocked and locked states for mode-A and mode-B can simultaneously overrun 30 dB, which

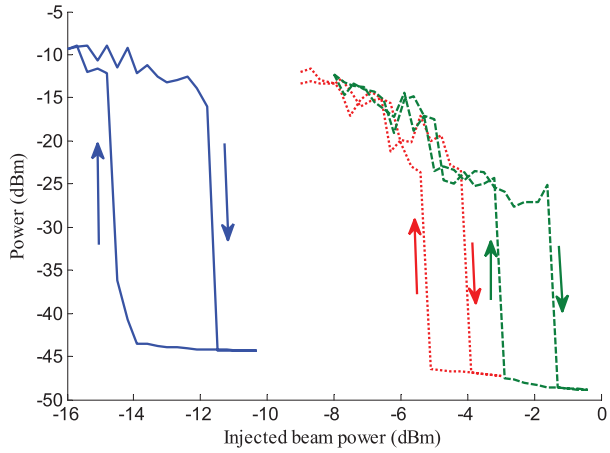

(a)

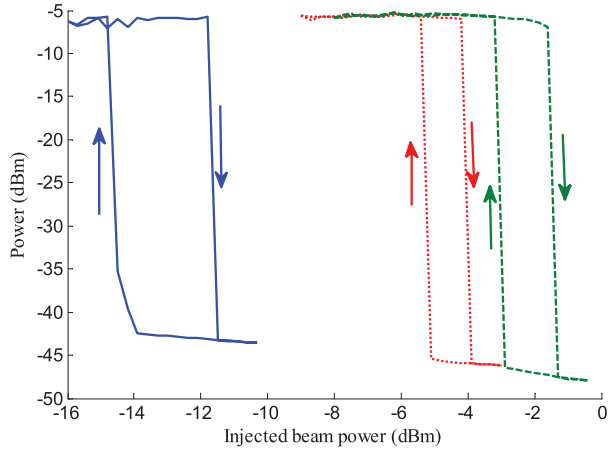

(b)

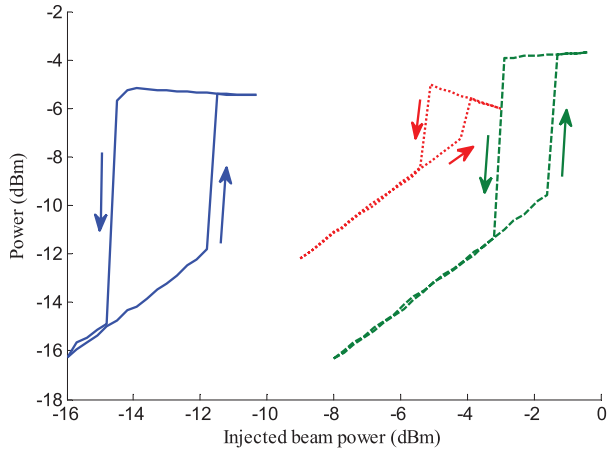

(c)

FIG. 6. Hysteresis loops caused by the externally injected power with wavelength detuning levels of 0.04 nm (blue solid line), 0.08 nm (red dotted line), and 0.12 nm (green dashed line) for (a) mode-A, (b) mode-B, and (c) the selected side mode.

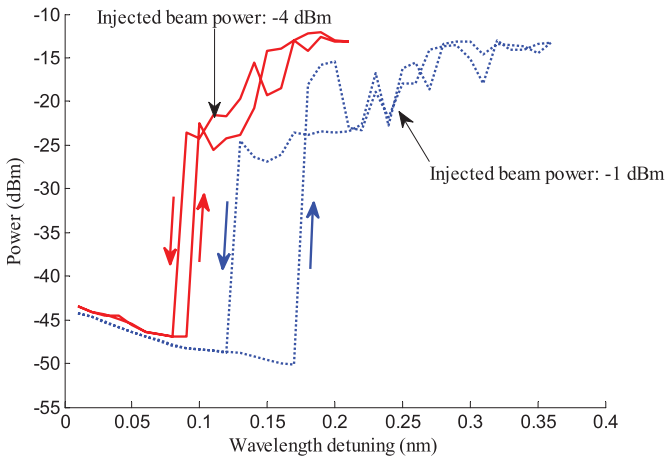

(a)

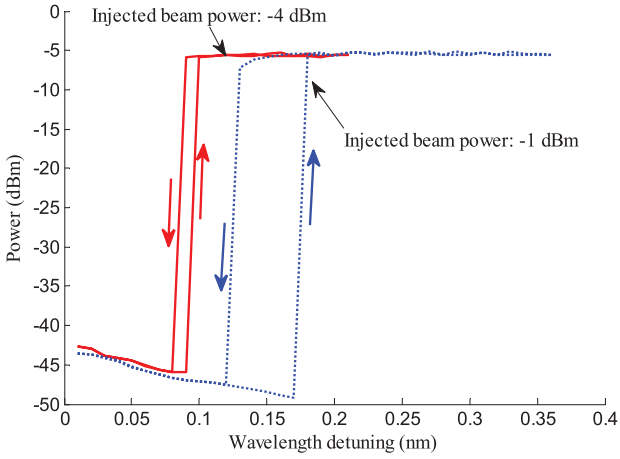

(b)

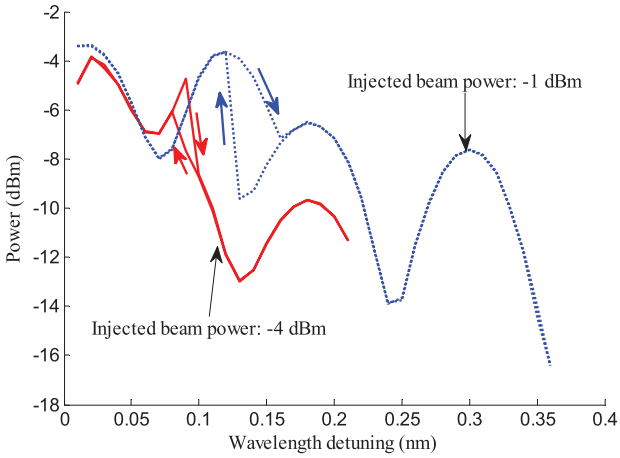

(c)

FIG. 7. Hysteresis loops caused by wavelength detuning for injected power levels of −4 dBm (red solid line) and −1 dBm (blue dotted line) for (a) mode-A, (b) mode-B, and (c) the selected side mode.

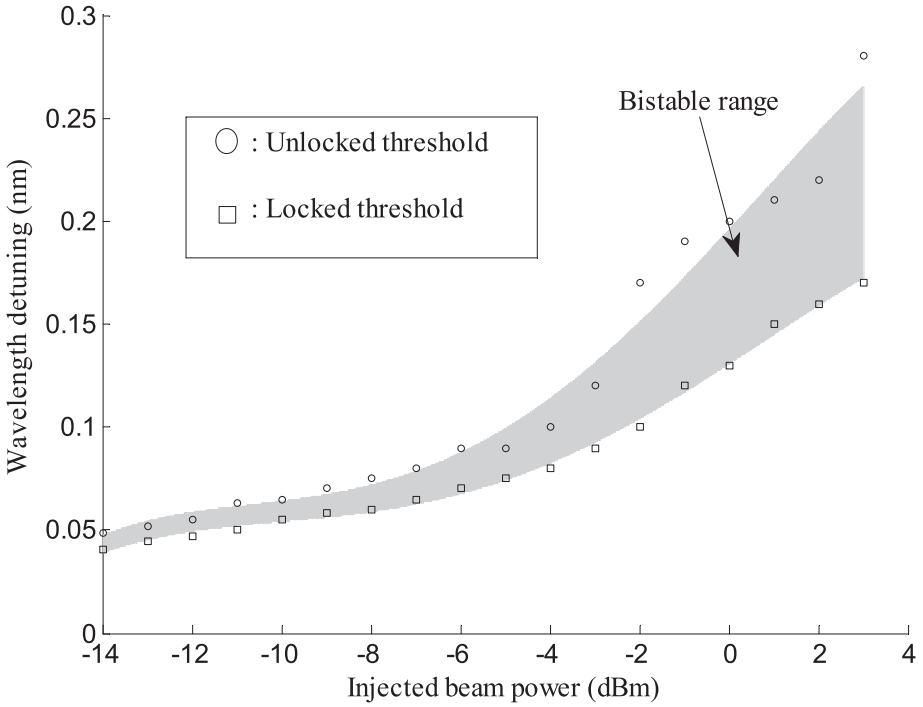

FIG. 8. Bistability range relative to injection power and wavelength detuning.

is further higher than the corresponding value for the selected side mode case shown in Fig. 6(c), and where we can also see that a counterclockwise hysteresis direction is shown in the bistability loop.

In the FP-LD laser system, a change in the level of wavelength detuning will also lead to hysteresis of the lasing mode under fixed injected power conditions that can cause the laser to be locked at the injected wavelength by means of the appropriate wavelength detuning. The bistability loop induced by wavelength detuning is plotted for two injected power levels of −4 dBm and −1 dBm in Fig. 7, in which we see that, with increasing injected power, the wavelength detuning related locking range gradually broadens, with the result that the output hysteresis loop width is obviously extended for the injected power of −1 dBm in comparison with that of the lower input power level (e.g. −4 dBm). In addition, mode-A still suffers the fluctuating behavior shown in Fig. 7(a) with the change in wavelength detuning. In contrast, Fig. 7(b) shows that mode-B has a more stable output state than that of mode-A with the change of wavelength detuning. In the bistability loops, counterclockwise hysteresis directions are observed for mode-A and mode-B, while a clockwise hysteresis direction is shown for the selected side mode in Fig. 7(c). In the loop displayed in Fig. 7(c), the captured power takes on an oscillating output state with increasing wavelength detuning because of the effect of the interference between the externally injected beam and the selected side mode.

Based on the above discussion and our proposed dual-mode laser system, we can see that bistability loops with various widths can be obtained by appropriate adjustment of the wavelength detuning and externally injected power. From these research results, we conclude that a wide hysteresis loop is better for optical memory operation, while high speed optical switching would be better with the narrow bistability loop. The output optical hysteresis is strongly dependent on the injected power and the wavelength detuning, with a bistability range that is shown with respect to the injected power and the wavelength detuning in Fig. 8, in which we can see that the narrowest loop width occurs at a wavelength detuning level of around 0.1 nm.

IV. CONCLUSIONS

We have experimentally demonstrated a dual-mode lasing system based on strict control of the drive current and operating temperature of a Fabry-Pérot laser diode with a built-in external cavity configuration. In contrast to SMFP-LDs, injected power and wavelength detuning dependent nonlinear behavior, including injection locking and optical stability, is observed in the DMFP-LD system demonstrated here and is discussed. After the externally injected power is introduced into the active region, as a result of the effects of mode competition, one of the two oscillation modes showed strong oscillation behavior because of the change in the injected power and the wavelength detuning before full injection locking occurred. The resulting contrast ratios of emission modes between the unlocked and locked states are simultaneously up to 30 dB. Following this study, the presented dual-mode lasing system will be applied to further study of potential applications, including optical memory and switching.

ACKNOWLEDGMENTS

This research was supported by a grant from the R&D Program (Industrial Strategic Technology Development) funded by the Ministry of Knowledge Economy (MKE) of the Republic of Korea and Open Fund of State Key Laboratory of Information Photonics and Optical Communications (Beijing University of Posts and Telecommunications).

[1] H. Maestre, A. J. Torregrosa, J. A. Pereda, C. R. Fernández-Pousa, and J. Capmany, "Dual-wavelength Cr^{3+}: $LiCaAlF_6$ solid-state laser with tunable THz frequency difference," IEEE J. Quantum Electron. **46**, 1681 (2010).
[2] M. Tang, H. Minamide, Y. Y. Wang, T. Notake, S. Ohno, and H. Ito, "Tunable terahertz-wave generation from DAST crystal pumped by a monolithic dual-wavelength fiber laser," Opt. Exp. **19**, 779 (2011).
[3] R. Braakman and G. A. Blake, "Principles and promise of Fabry-Pérot resonators at terahertz frequencies," J. Appl. Phys. **109**, 063102 (2011).
[4] A. Klehr, J. Fricke, A. Knauer, G. Erbert, M. Walther, R. Wilk, M. Mikulics, and M. Koch, "High-power monolithic two-mode DFB laser diodes for the generation of THz radiation," IEEE J. Sel. Topics Quantum Electron. **14**, 289 (2008).
[5] C. S. Friedrich, C. Brenner, S. Hoffmann, A. Schmitz, I. C. Mayorga, A. Klehr, G. Erbert, and M. R. Hofmann, "New two-color laser concepts for THz generation," IEEE J. Sel. Topics Quantum Electron. **14**, 270 (2008).
[6] T. Kleine-Ostmann, P. Knobloch, M. Koch, S. Hoffmann, M. Breede, M. Hofmann, G. Hein, K. Pierz, M. Sperling, and K. Donhuijsen, "Continuous-wave THz imaging," Electron. Lett. **37**, 1461 (2001).
[7] T. Nagatsuma, "Radio spectral evolution with photonics," International topical meetings on microwave photonics/Asia-Pacific Microwave photonics conference, Gold Coast, Australia, 2008.
[8] Y. F. Wu, C. H. Yeh, C. W. Chow, F. Y. Shih, and S. Chi, "Employing external injection-locked Fabry-Pérot laser scheme for mm-wave generation," Laser Phys. **21**, 718 (2011).
[9] J. Huang, C. Z. Sun, B. Xiong, and Y. Luo, "Y-branch integrated dual wavelength laser diode for microwave generation by sideband injection locking," Opt. Exp. **17**, 20727 (2009).
[10] G. E. Villanueva, J. Palací, J. L. Cruz, M. V. Andrés, J. Martí, and P. Pérez-Millán, "High frequency microwave signal generation using dual-wavelength emission of cascaded DFB fiber lasers with wavelength spacing tunability," Opt. Commun. **283**, 5165 (2010).
[11] C. H. Chen, S. Matsuo, K. Nozaki, A. Shinya, T. Sato, Y. Kawaguchi, H. Sumikura, and M. Notomi, "All-optical memory based on injection-locking bistability in photonic crystal lasers," Opt. Exp. **19**, 3387 (2011).
[12] P. Heinricht, B. Wetzel, S. O'Brien, A. Amann, and S. Osborne, "Bistability in an injection locked two color laser with dual injection," Appl. Phys. Lett. **99**, 011104 (2011).
[13] S. Osborne, K. Buckley, A. Amann, and S. O'Brien, "All-optical memory based on the injection locking bistability of a two-color laser diode," Opt. Exp. **17**, 6293 (2009).
[14] N. Brandonisio, P. Heinricht, S. Osborne, A. Amann, and S. O'Brien, "Bistability and all-optical memory in dual-mode diode lasers with time-delayed optical feedback," IEEE Photon. J. **4**, 95 (2012).
[15] J. M. Mehta, "Dual wavelength interferometric technique for simultaneous temperature and concentration measurements in liquids," Appl. Opt. **29**, 1924 (1990).
[16] V. Gusmeroli and M. Martinelli, "Two-wavelength interferometry by superluminescent source filtering," Opt. Commun. **94**, 309 (1992).
[17] V. Ménoret, R. Geiger, G. Stern, N. Zahzam, B. Battelier, A. Bresson, A. Landragin, and P. Bouyer, "Dual-wavelength laser source for onboard atom interferometry," Opt. Lett. **36**, 4128 (2011).
[18] S. Osborne, P. Heinricht, N. Brandonisio, A. Amann, and S. O'Brien, "Wavelength switching dynamics of two-colour semiconductor lasers with optical injection and feedback," Semicond. Sci. Technol. **27**, 094001 (2012).
[19] H. Kim, P. van der Wal, A. Schmitz, and R. Güsten, "Power stabilization of the dual-mode laser using volume holographic gratings," J. Lightwave Technol. **26**, 1317 (2008).
[20] Z. Li, J. Zhou, B. He, H. K. Liu, C. Liu, Y. R. Wei, J. X. Dong, and Q. H. Lou, "Controllable dual-wavelength fiber laser," Chin. Phys. Lett. **29**, 074203 (2012).

[21] F. Grillot, N. A. Naderi, J. B. Wright, R. Raghunathan, M. T. Crowley, and L. F. Lester, "A dual-mode quantum dot laser operating in the excited state," Appl. Phys. Lett. **99**, 231110 (2011).
[22] S. Latkowski, J. Parra-Cetina, R. Maldonado-Basilio, P. Landais, G. Ducournau, A. Beck, E. Peytavit, T. Akalin, and J. F. Lampin, "Analysis of a narrowband terahertz signal generated by a unitravelling carrier photodiode coupled with a dual-mode semiconductor Fabry-Pérot laser," Appl. Phys. Lett. **96**, 241106 (2010).
[23] S. M. Nekorkin, A. A. Biryukov, P. B. Demina, N. N. Semenov, B. N. Zvonkov, V. Y. Aleshkin, A. A. Dubinov, V. I. Gavrilenko, K. V. Maremyanin, S. V. Morozov, A. A. Belyanin, V. V. Kocharovsky, and V. V. Kocharovsky, "Nonlinear mode mixing in dual-wavelength semiconductor lasers with tunnel junctions," Appl. Phys. Lett. **90**, 171106 (2007).
[24] I. Park, I. Fischer, and W. Elsäßer, "Highly nondegenerate four-wave mixing in a tunable dual-mode semiconductor laser," Appl. Phys. Lett. **84**, 5189 (2004).
[25] J. Hörer and E. Patzak, "large-signal analysis of all-optical wavelength conversion using two-mode injection-locking in semiconductor lasers," IEEE J. Quantum Electron. **33**, 596 (1997).
[26] K. Y. Park, S. G. Mun, K. M. Choi, and C. H. Lee, "A theoretical mode of a wavelength-locked Fabry-Pérot laser diode to the externally injected narrow-band ASE," IEEE Photon. Technol. Lett. **17**, 1797 (2005).
[27] H. K. Tsang, L. Y. Chan, S. P. Yam, and C. Shu, "Experimental characterization of dual-wavelength injection-locking of a Fabry-Pérot laser diode," Opt. Commun. **156**, 321 (1998).
[28] Y. D. Jeong, Y. H. Won, S. O. Choi, and J. H. Yoon, "Tunable single-mode Fabry-Pérot laser diode using a built-in external cavity and its modulation characteristics," Opt. Lett. **31**, 2586 (2006).
[29] M. Rakib-Uddin and Y. H. Won, "All-optical wavelength conversion by the modulation of self-locking state of a single-mode FP-LD," IEEE Photon. Technol. Lett. **22**, 290 (2010).
[30] B. Nakarmi, M. Rakib-Uddin, T. Q. Hoai, and Y. H. Won, "Demonstration of all-optical NAND gate using single mode Fabry-Pérot laser diode," IEEE Photon. Technol. Lett. **23**, 236 (2011).
[31] N. L. Hoang, J. S. Cho, Y. H. Won, and Y. D. Jeong, "All-optical flip-flop with high on-off contrast ratio using two injection-locked single-mode Fabry-Pérot laser diodes," Opt. Exp. **15**, 5166 (2007).
[32] B. Nakarmi, M. Rakib-Uddin, T. Q. Hoai, and Y. H. Won, "A simple controlled all-optical on/off switch using gain modulation in single mode FP-LD," IEEE Photon. Technol. Lett. **23**, 212 (2011).
[33] R. I. Álvaren-Tamayo, M. Durán-Sánchez, O. Pottiez, B. Ibarra-Escamilla, J. L. Cruz, M. V. Andrés, and E. A. Kuzin, "A dual-wavelength tunable laser with superimposed fiber Bragg gratings," Laser Phys. **23**, 055104 (2013).
[34] J. W. Wu, B. Nakarmi, T. Q. Hoai, and Y. H. Won, "Tunable two-color lasing emission based on Fabry-Pérot laser diode combined with external cavity feedback," IEEE Photon. J. **5**, 1500108 (2013).
[35] L. Q. Yu, D. Lu, L. J. Zhao, Y. Li, C. Ji, J. Q. Pan, H. L. Zhu, and W. Wang, "Wavelength and mode-spacing tunable dual-mode distributed Bragg reflector laser," IEEE Photon. Technol. Lett. **25**, 576 (2013).
[36] Y. X. Xiang, X. Z. Zhang, W. Cai, L. Wang, C. F. Ying, and J. J. Xu, "Optical bistability based on Bragg grating resonators in metal-insulator-metal plasmonic waveguides," AIP Adv. **3**, 012106 (2013).
[37] S. Roshan Entezar, "Optical bistability in one-dimensional photonic band gap structure with nonlinear graded-index defect layer," Opt. Commun. **287**, 19 (2013).
[38] S. Chiangga, S. Pitakwongsaporn, T. D. Frank, and P. P. Yupapin, "Optical bistability investigation in a nonlinear silicon microring circuit," J. Lightwave Technol. **31**, 1101 (2013).